

Supplementary Data

Modeling (Figure 7)

The model presented in Figure 7 is simplified in several respects. Cocaine is shown to bind only to the T_oNaCl intermediate, conversion of T_i and T_o is shown as an electrogenic step and there is a binding order implied for Na^+ , Cl^- and 5-HT. However, we know that 5-HT and cocaine can bind in the absence of Na^+ and Cl^- (1,2) and that transport is electroneutral because H^+ is transported in the absence of K^+ (3). To accurately represent these complexities, a diagram showing intermediates such as T_oS , T_oCl , T_oScl and T_oNaS would be needed, in addition to T_oCoc , T_oNacoc and T_oClcoc . We would also need T_iH and T_oH intermediates in accordance with the known antiport of H^+ in the absence of internal K^+ (3). To avoid an overly complex model that would be difficult to follow, we made simplifications to the full mechanism in the model shown in Figure 7. However, the ability of the model to account for the measured currents does not depend on the binding order of Na^+ , Cl^- or 5-HT under physiological conditions. Possible shortcomings of the model (e.g a false binding order) would become apparent only under non-physiological conditions (e.g removal of Cl^- or Na^+). Similarly modeling based on our assignment of T_oNaCl as the cocaine-binding intermediate is indistinguishable from a model including Cl^- independent cocaine binding as long as Cl^- is present. Had we assigned cocaine binding to the T_oNa intermediate in our sequential scheme, the model would falsely predict that Cl^- and cocaine could not bind to the transporter simultaneously.

Modeling of ibogaine binding rates (Figure 7c)

For a pseudo first order binding reaction as assumed for ibogaine, the linear fit shown in 6d provides the k_{on} (slope) and the k_{off} (y-intercept) for binding. These parameters allow calculation of ibogaine's K_D , which can be compared with the values obtained in steady state (Figure 3a,b). However our simulation (see supplementary Figure S4) predicts that an increase in the time for solution exchange will decrease the slope (compare instantaneous exchange, $\tau_{on}=0$ ms with the $\tau_{on}=50$ ms line). This decrease is consistent with the observed mismatch between the K_D calculated from Figure 6d ($\sim 60 \mu M$) and the K_D measured by transport inhibition ($\sim 6 \mu M$). When we accounted for non-instantaneous solution exchange we also saw a small deviation from a strictly linear behavior (7c) that was not apparent in the measured data (6d). It is possible that this deviation was present in our data but was obscured by the uncertainty of the measurement.

Supplementary Figures

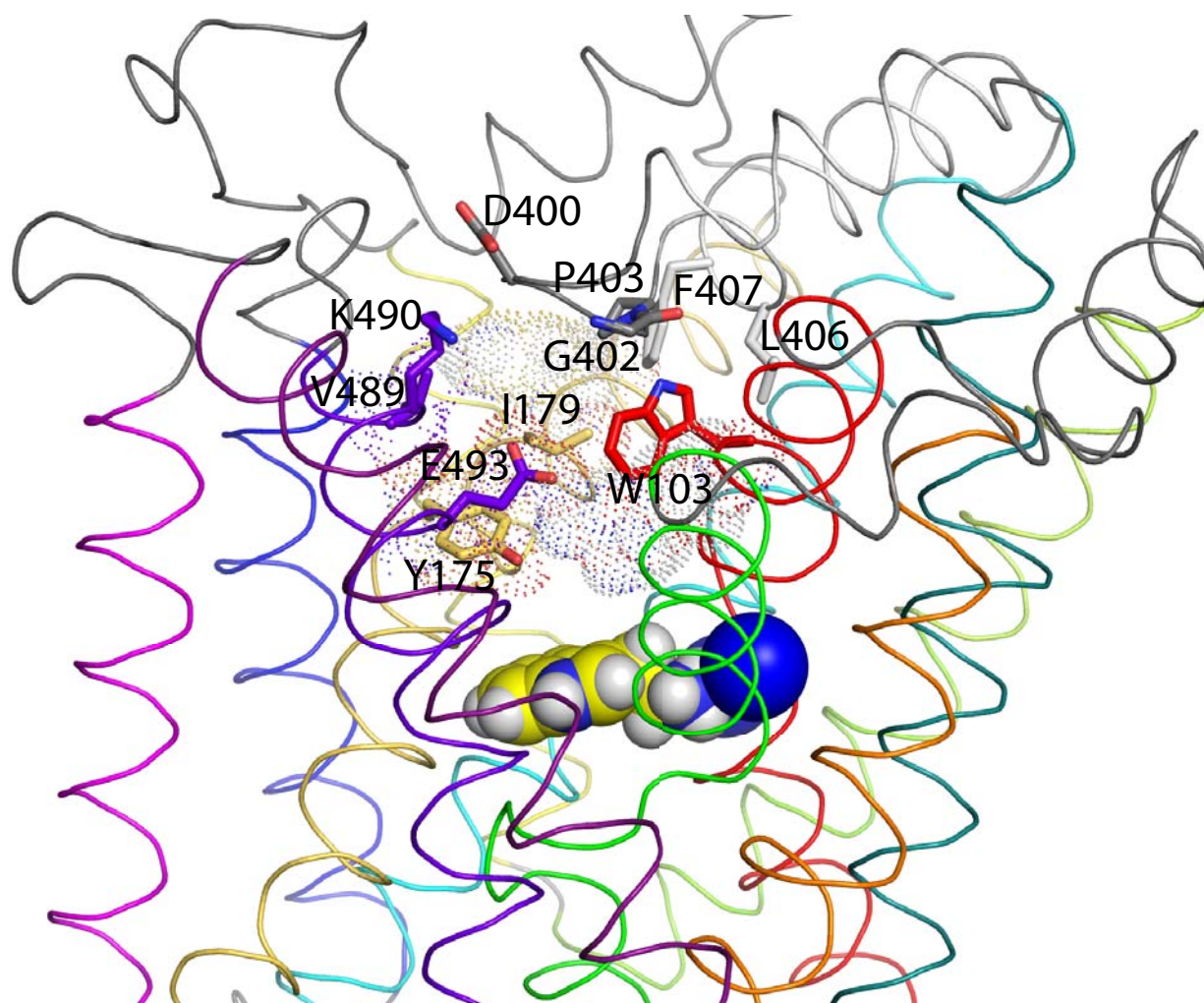
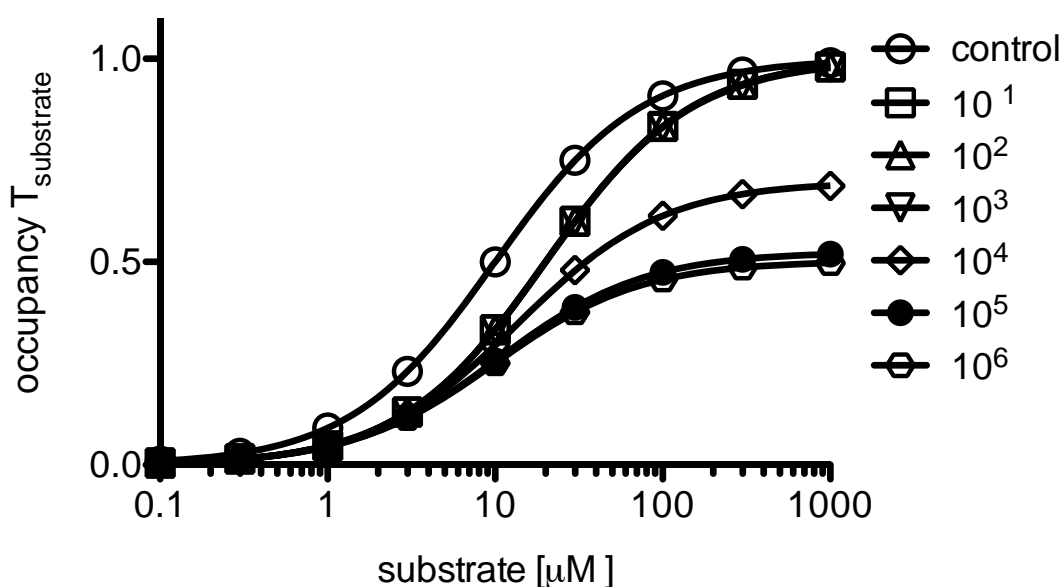


Figure S1. Mutations that failed to decrease ibogaine potency. A homology model of SERT based on the occluded (2A65) structure of LeuT (4) is shown, with the α -carbon chain in ribbon representation with color coding as in (4). 5-HT (yellow) and Na^+ (blue) are shown as spheres, and the side chains of mutated residues are shown as sticks and labeled. Positions corresponding to the S2 site described for DAT (5) are shown as dots.

(a)



(b)



	control	10 ¹	10 ²	10 ³	10 ⁴	10 ⁵	10 ⁶
Bmax	1.000	1.000	1.000	0.9970	0.6975	0.5244	0.5025
Kd	9.999	20.00	20.00	19.91	13.71	10.48	10.05

Figure S2. Analysis of how slow dissociation of an inhibitor could appear as non-competitive inhibition. A. Simple model of substrate and inhibitor binding to the same intermediate. B. Plotted is the occupancy of $T_{\text{substrate}}$ as a function of the substrate concentration. The inhibitor was allowed to equilibrate with its binding site prior to the addition of substrate. The plotted data points are the occupancy of $T_{\text{substrate}}$ that was reached after 60 seconds of substrate application. The curve labeled control is a simulation in the absence of inhibitor. All other simulations are in the presence of 1 μM inhibitor (K_D). Different $k_{\text{off}}^{\text{substrate}}/k_{\text{off}}^{\text{inhibitor}}$ ratios were tested (101,102,103,104,105,106). The data points were fit to a one site-binding model and the fit parameters Bmax and apparent K_D are displayed in the table

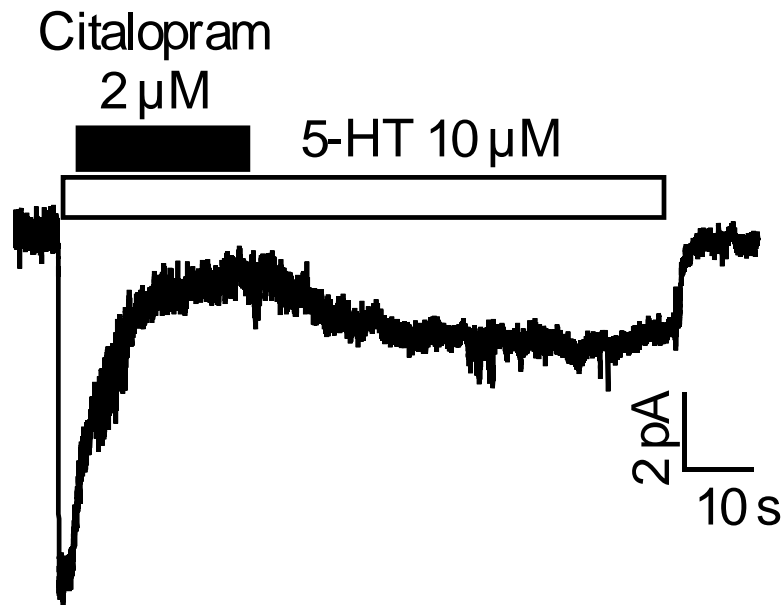


Figure S3. Slow binding and dissociation of citalopram. Time course of citalopram blockade of the 5-HT current was determined in single SERT-expressing HEK-293 cells as shown for ibogaine and cocaine in Figure 5 a and b.

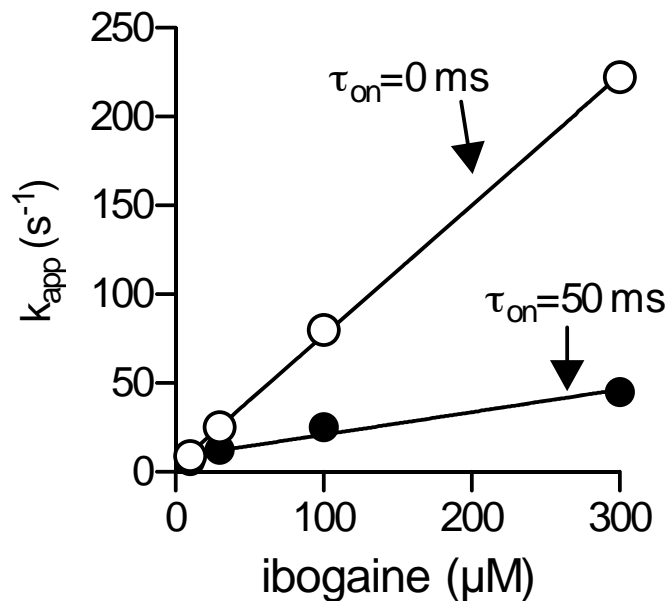


Figure S4. Simulation of ibogaine blocking kinetics depends on the rate of solution exchange. Shown are the simulated k_{app} values for ibogaine block of substrate induced current as a function of the ibogaine concentration. One simulation was conducted assuming instantaneous solution exchange. In this case the concentration of ibogaine over time followed a step function ($\tau_{on}=0$ ms). In a second simulation ibogaine concentration over time was modeled to rise exponentially with a time constant of 50 ms, to account for the speed of the superfusion device used in our measurements.

Supplementary References

1. Humphreys, C. J., Wall, S. C., and Rudnick, G. (1994) *Biochemistry* **33**, 9118-9125
2. Tavoulari, S., Forrest, L. R., and Rudnick, G. (2009) *J. Neurosci.* **29**, 9635-9643
3. Keyes, S. R., and Rudnick, G. (1982) *J. Biol. Chem.* **257**, 1172-1176
4. Yamashita, A., Singh, S. K., Kawate, T., Jin, Y., and Gouaux, E. (2005) *Nature* **437**, 215-223
5. Shan, J., Javitch, J. A., Shi, L., and Weinstein, H. (2011) *PLoS One* **6**, e16350